An Investigation of CFRP Laminates Cured in a Commercial Toaster Oven: Quality and Economic Assessment

Pimpet Sratong-on[1] Titirat Vivithkeyoonvong[2] Sutep Joy-A-Ka[3] Sawanya Suwannawong[4*]

[1,4*]*Composite Materials and Lightweight Structures Laboratory, Faculty of Engineering, Thai-Nichi Institute of Technology, Bangkok, Thailand*

[2]*Advanced Mobility and Propulsion Research Laboratory, Faculty of Engineering, Thai-Nichi Institute of Technology, Bangkok, Thailand*

[3]*Materials Properties and Failure Analysis Laboratory, Thailand Institute of Scientific and Technological Research, Pathum Thani, Thailand*

*Corresponding Author. E-mail address: sawanya@tni.ac.th

Received: 19 July 2024; Revised: 12 November 2024; Accepted: 12 November 2024
Published online: 26 December 2024

Abstract

This study demonstrated the ability to produce high-quality carbon fiber-reinforced plastic (CFRP) laminates with low void contents using a single cure cycle setting up in commercial toaster oven via Vacuum-Bag-Only (VBO) process. The results were discussed in quality and economic views. X-ray micro-CT 3D images of the resulting laminates revealed the 0.28% void content; therefore, it can be classified as very good quality by Purslow chart. Tensile (ASTM D3039) and flexural (ASTM D790) tests were conducted and the results were compared to void-free laminate considered in finite element analysis. The high tensile and flexural strength of laminates were 451.02 MPa and 767.61 MPa, respectively, which were only 12.12% less than simulation results. The cost analysis was conducted to investigate the breakeven point of commercial toaster oven, autoclave and industrial thermal oven for curing CFRP. The results disclosed that the autoclave contributed the highest oven cost and electricity cost. The breakeven point of commercial toaster oven was 54,000 pieces of similar size of CFRP laminate curing by industrial thermal oven. This suggested that commercial toaster oven was economical choice for moderate production capacity and small working place.

***Keywords*:** Carbon fiber-reinforced plastic (CFRP), Mechanical properties, Vacuum-bag-only process (VBO), Void content, X-ray micro-CT

I. INTRODUCTION

Carbon fiber-reinforced plastic (CFRP) has been used as a lightweight material in the aerospace and automotive industries, as well as in the construction of sports equipment due to its high strength-to-weight ratio and its resistance to corrosion compared to metal. For the automobiles, lighter vehicles consume less energy, allowing vehicles to travel longer distances with lower emission of CO2 [1]–[3]. Consequently, one of the main challenges for the automotive industry is to design lightweight vehicles using CFRP and/or other lightweight materials. Several studies have proposed the use of CFRP as a substitute for metallic parts or mixed with metals to enhance their strength-to-weight ratio and crashworthiness [4]–[6]. Nevertheless, unlike metals, an isotropic material, CFRP is an anisotropic material, making their mechanical properties are strongly dependent on the orientation of fibers [7], [8].

The fabrication of CFRP involves the hand lay-up of the carbon fiber to align the fibers in a desired direction, followed by curing of the thermoset or thermoplastic resins. In the aerospace industry, an autoclave oven is commonly used for the consolidation of CFRP since it allows for high pressures to be applied during curing process at elevated temperatures. Therefore, the autoclave process can achieve extremely low void contents (0–1%) while maintaining a 55–65% fiber fraction [9]. However, the high initial investment costs, severe maintenance requirements, long production times, and the large size of the autoclave lead to a high-cost manufacturing process with finite manufacturing capacities. Saenz-Castillo *et al.* studied the effect of consolidation cycles of three different out-of-autoclave (OOA) processes—Vacuum-Bag-Only (VBO), hot-press, and automatic lay-up with in-situ consolidation—on the void content and mechanical properties of carbon fiber/PEEK composites [10]. The in-plane and interlaminar shear strength of the materials rapidly decreased once the void content was higher than 1.2%, 1.6%, and 2.7% for VBO, automatic lay-up with in-situ consolidation, and hot-press, respectively. Hence, it is demonstrated that VBO processes can achieve the low void contents necessary to produce CFRPs with improved mechanical properties. The detailed comparisons of autoclave and VBO processes with different curing methods, percentage of void content in CFRP laminate after curing and mechanical properties are summarized in Table 1.

Table 1: Comparison of autoclave and VBO process

Features	Autoclave	VBO	
		Thermal industrial curing oven	Microwave curing
Curing Pressure	0.3–0.7 MPa [11]–[13]	Atmospheric pressure	Atmospheric pressure
Curing time	≥ 480 min [14]	≥ 700 min [15]	≥ 271 min [16]
Curing step	2–8 [16], [17]	≥2 [9]	≥2 [16]
Part size	Length of 27 m [16]	0.1–2.5 m^2 [15]	Only small size [18]
Acheivable thickness	32 plies, 4.15 mm [19]	16 plies, 2.16 mm [10]	4 plies, 2.8 mm [20]
Void Content	0.0–1.0% [9]	0.5–3.0% [9]	8.9% [18]
In-plane shear strength	108.01 MPa [9]	111.36 MPa [9]	45.0 ± 4.05 MPa [21]
Energy consumption [16]	Vacuum: 1.3 kW•h Curing: 37.4 kW•h	Vacuum: 2.1 kW•h Curing: 10.8 kW•h	Vacuum: 1.8 kW•h Curing: 14.4 kW•h
Overhead cost [16]	252 $/ process	215 $/hr	254 $/ process

VBO process uses the vacuum-bag pressure (typically -1 bar) to compact the pre-impregnated fibers (prepreg). The VBO process allows for the curing of prepreg over a diverse range of equipment, including thermal convection ovens, heat blankets, and microwave ovens

[22]–[24]. Among these curing techniques, thermal convection oven methods exhibited the lowest costs, cycle times, and energy requirements. Centea and Nutt conducted a technical cost analysis of the manufacturing costs of a VBO prepreg process followed by curing in a thermal convection oven and found that prepreg processing was the greatest contributor to material costs, while the oven accounted for most of the equipment costs [15]. Nevertheless, the cure cycle of a CFRP laminate produced a VBO process using a convection thermal oven needs at least two steps: 1) a low-temperature curing, involving TB (B-stage curing) with a first isothermal hold for t_B seconds; and 2) a high-temperature curing, T_C (C-stage curing) with a second isothermal hold for t_C seconds [25]. During B-stage curing, the volatiles, i.e,. gas and reaction by-product of resin, are free to escape with sufficient dwell time and appropriate temperature and provide the rest of flowable resin for C-stage curing. In the autoclave process, the pressure is applied to consolidate the laminate, and the rest of flowable resin can fill the air gap between plies. For the OOA process, the resin is fully cured by the elevated temperature, allowing the consolidation of laminate. The total cure cycle time for VBO process by a thermal convection oven is approximately 700 minutes, which still represents a relatively long production cycle. The comparison of fabrication conditions, energy consumption and overhead cost between autoclave and VBO process are summarized in Table 1. Since at least two steps of the cure cycle are necessary to cure VBO-generated CFRP laminates in thermal convection ovens, this necessitates the installation of complicated controller systems within the thermal ovens. Thus, composite curing ovens used in VBO processes are generally made-to-order; consequently, the initial cost of procuring this equipment is still expensive and unaffordable for many small entrepreneurs compared to commercial ovens that are widely available in both physical department stores and online marketplaces.

To the best of the authors' knowledge, the use of commercial ovens for the curing of CFRP laminates generated by VBO processes has not been demonstrated elsewhere. This study aims to demonstrate the use of commercial toaster ovens for the curing of CFRP laminates produced by VBO process. Due to the limited controls available to commercial toaster ovens, only a single cycle can be implemented: a single temperature ramp followed by an isothermal hold. The curing temperature at the final stage of vacuum bag curing, 120ºC, and holding for 50 mins was selected as recommended by the manufacturer [17]. The mechanical properties; tensile and flexural tests, were conducted on the [0/90/0/90] CFRP laminate fabricated by VBO process with and without vacuum atmosphere and compared with finite element analysis due to negligible voids in laminate. The surface and through-thickness voids were investigated by digital microscope and X-ray micro-CT, respectively. The cost analysis was performed, and the break-even point was determined to investigate the economic alternatives between autoclave, industrial curing oven, and commercial toaster oven.

II. PREPARATION OF THE CFRP LAMINATE USING A COMMERICAL TOASTER OVEN

A. Toaster Oven Setup

A 290 × 460 × 280 mm^3 commercial toaster oven (Model No. OTTO TO-765, OTTO Kingglass Co. Ltd., Thailand); Figure 1a), was used to cure the CFRP laminate. The direction of heat flow in the oven was adjusted to flow from the top and bottom of the oven (Figure 1a), allowing the middle section of the oven to be maintained at an average temperature that was roughly equivalent to the set temperature. A temperature sensor was placed in the middle of the oven before fabrication to monitor the temperature in this section

of the oven (Figure 1b). The temperature of the oven was set to 120°C, while the timer was set to 50 mins. An alarm went off once the temperature in the oven reached 120°C. It was found that the oven took 40 mins to reach 120°C from the room temperature (22°C), indicating that the commercial toaster oven had a heating rate of 2.5°C/min, which falls within the range of heating ramp rates recommended for curing as indicated by the manufacturer [17].

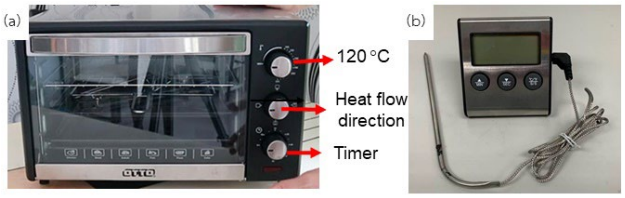

Figure 1: Equipment used for the VBO process used in this study: (a) Toaster oven and (b) temperature sensor.

B. Fabrication Procedures

A 200 g/m^2 2 × 2 plain weave of carbon fiber prepreg consisting of 58 vol.% carbon fiber (Tenax HTA-3k) and 42 vol.% epoxy resin (DT806R; DeltaPreg, Italy) was used to fabricate a 120 × 240 mm^2 CFRP laminate with a stacking sequence of [0/90/0/90]. The non-vacuum specimen was used to investigate the maximum void content that could be obtained when the specimen was cured using a commercial toaster oven. The VBO accessories used in the experimental setup consisted of a release film, breather, vacuum bagging film, and carbon fiber laminate; these were arranged in order as shown in Figure 2a. The bagging film was then attached using sealant tape. For the specimen cured under vacuum, the apparatus was directly connected to the vacuum pump using a vacuum connector. Once the vacuum pressure (-1 bar) was reached, the vacuum pump was allowed to run continuously for 1 min before being turned off. This process was repeated 1–3 times until no additional air leakage was observed. The air leakage can be observed by the return of the needle in pressure gage to atmospheric pressure. The carbon fiber laminate was cured at 120°C for 50 minutes, followed by cooling at room temperature. It was found that the final CFRP laminate product had a nominal thickness of 1 mm as shown in Figure 2b. The fabrication procedures used for the non-vacuum specimen were the same as the methods described above except that the vacuum pump was not used.

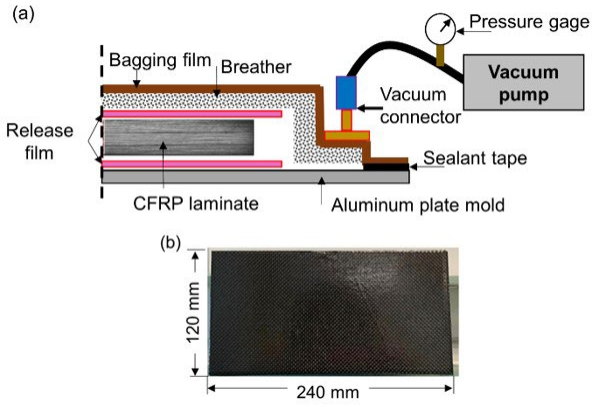

Figure 2: The fabrication process of the CFRP laminates: (a) schematic diagram of the VBO process used for the vacuum specimens; (b) an image of the final CFRP laminate cured under vacuum conditions.

III. FINITE ELEMENT (FE) MODELLING

Finite element analysis (FEA) typically neglects the presence of voids in CFRP specimens. Consequently, the results of a FEA should give an upper bound of the mechanical performance of the CFRP specimens. This study used the ANSYS Composite PrepPost (ACP) module in the ANSYS finite element software to model the CFRP specimens. Figures 3a and 3b illustrate the boundary conditions of the tensile and three-point bending tests, respectively. In the tensile test, one side of the CFRP was clamped. The other side of the specimen was used to exert tension along the y-axis by the applied displacement $\Delta\delta_y$. In the three-point bending test, no translation was allowed along the x-, y-, and z-axes in the left support, while no translation was allowed along the y- and z-axes in the right

support. The displacement, $\Delta\delta_y$, pointed in opposite direction to the y-axis at the middle of the specimen (i.e., at a distance of $L_s/2$) to perform three-point bending test. In both mechanical tests, the displacement was increased until the CFRP laminate failed under the Tsai-Wu failure criteria. The element size used in the FE model of the tensile and three-point bending tests was 2 mm, resulting in 726 elements and 854 nodes. The material constants of the carbon fiber prepreg (Tenax HTA-3k DT806R) used in the FE model are presented in Table 2.

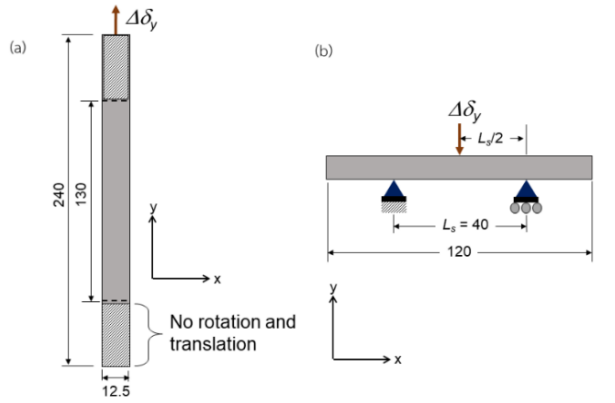

Figure 3: The boundary conditions for the FE model used to simulate the mechanical tests of the CFRP laminates: (a) the tensile test (ASTM D3039) and (b) the three-point bending test (ASTM D790). All dimensions are in mm.

Table 2: Material constants of CFRP for FE modeling [17]

E_x (GPa)	56.6	Density (kg/m^3)	1760
E_y (GPa)	56.6	G_{xy} (GPa)	3.5
E_z (GPa)	5.6	G_{yz} (GPa)	2.85
v_{xy}	0.04	G_{xz} (GPa)	2.85
v_{yz}	0.3	Areal weight (g/m^2)	200
v_{xz}	0.3	Nominal thickness (mm)	0.25

IV. CHARACTERIZATION OF THE MATERIALS

A. Investigation of Surface Apperance and Through-thickness Voids

The surface appearance of CFRP laminate was examined at a 2000× magnification using a digital microscope (BM-DM61, Ningbo Barride Optics Co., Ltd., China). Since the table of the digital microscope was too small to allow for the observation of the 120 × 240 mm CFRP laminate, each specimen was cut into six 12.5 × 240 mm pieces using an advanced composite plate saw (EXTEC Labcut® 5000, Extec Corp, USA). These smaller-sized specimens were also used in the tensile tests (ASTM D3039 standard). The CFRP specimens were scanned using an X-ray micro-CT (Skyscan, 1273, Bruker, USA) to examine the properties of the through-thickness voids. The specimen was scanned under 40 kV and 300 µA conditions with a 2 × 2 binning mode, 4 frames per projection, and a rotation step of 0.4°. The scan resolution (voxel size) was set to 12.0 µm. The X-ray micro-CT system was then used to reconstruct the 3D image. Due to specimen size limitations, the CFRP laminates were cut into 12.5 × 12.5 × 1.0 mm pieces for X-ray micro-CT scanning to ensure a scanning resolution of 12.0 µm. The distribution of the through-thickness voids in the CFRP laminates was found to be non-uniform along the length of the specimen [26], [27]. To ensure that the small portion of CFRP specimen scanned by X-ray micro-CT in this study was sufficiently representative of the void content of the entire sample, the error (e) of the deviation of the void content measured from smaller samples compared to the larger sample was determined by the following equation based on the work of Zhang *et al.* [28]:

$$e = \frac{|m - v|}{v} \quad (1)$$

where, m [%] and v [%] represent the void content of the small and large specimens, respectively.

While the width of the large sample was similar to that of the small CFRP specimen scanned by X-ray micro-CT, the length of the sample needed to be as large as possible for CCD camera detection. Consequently, the large sample cut from the CFRP laminate had dimensions of 12.5 × 180 mm. The larger specimen was scanned under the same conditions and resolutions used for the small specimens. It should be noted that

only the large specimen fabricated under vacuum was scanned as it was anticipated that the vacuum specimens would have a lower void content compared to the non-vacuum specimens, which was highly recommended for practical uses.

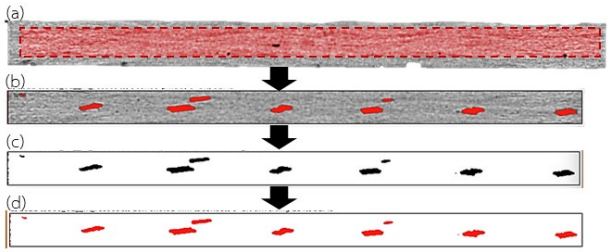

Figure 4: The workflow used to analyze the area of the through-thickness voids in the CFRP specimen using X-ray micro-CT imaging: (a) The image is cropped to exclude surface voids; (b) an appropriate threshold value is selected; (c) the 'Analyse Particles' function is used to highlight the void areas; (d) the area of voids in each slice is calculated.

B. An Analysis of Through Thickness Void Content Using X-ray Micro-CT Imaging

The ImageJ software was used to analyze the void content of the CFRP laminates in this study. All of the image stacks were imported and changed to an 8-bit image. Figure 4 presents the procedure used to analyze the through-thickness voids of the CFRP specimen from X-ray micro-CT images. First, the upper layer of each image was cropped to exclude voids on the surface of the specimens (Figure 4a). The voids created by air bubbles are presented in a dark black color compared to voids in the carbon fiber and matrix. Therefore, threshold range of 0–60 was used to visualize the area of the voids in the CFRP specimen and marked with the red coloring in Figure 4b. The 'Analyze Particles' mode was used to determine the area defined by this threshold (Figure 4c). The total void area in each slice, A_{void_slices}, was determined and multiplied by the thickness of each slice, t_{slice}, which was equal to the scanning resolution. The void content of the specimen, V_{void_slice}, could then be determined as follows:

$$V_{void\_slice} = \frac{A_{void\_surface} \times t_{slice}}{V_{total}} \times 100\% \quad (2)$$

where V_{total} [mm^3] is the total volume of the specimen, which can be determined by:

$$V_{total} = A_{crop} \times N_{slice} \times t_{slice} \quad (3)$$

where A_{crop} [mm^2] and N_{slice} [-] are the cropped area of each slice and the total number of slices, respectively.

C. Mechanical Tests

The mechanical tensile and flexural tests were conducted based on ASTM D3039/D3039M-00 and ASTM D790-03 standards, respectively [29], [30]. A universal testing machine (Zwick Roell, Z100SH, Germany) was used to perform tensile and flexural tests in three-point bending mode. Five 12.5 × 240 mm CFRP specimens with a gauge length of 130 mm were used in the tensile test with 0.01 min^{-1} strain rate. The ultimate tensile strength and tensile modulus were evaluated based on stress-strain curves. The percentage of elongation, %EL, was determined using Equation (4):

$$\%EL = \left(\frac{\ell - \ell_0}{\ell_0} \right) \times 100\% \quad (4)$$

where ℓ is the gauge length of specimen under tension [mm] and ℓ_0 is the original gauge length of specimens [mm]. The ultimate tensile strength, tensile modulus, and percentage of elongation at break of both vacuum and non-vacuum specimens were plotted and compared with the FE results. 12.5 × 120 mm specimens with a 32 mm span length, L_s, were used for the three-point bending test; these samples were tested at a strain rate of 0.01 min^{-1}. Since the size of the specimens used in the three-point bending test was smaller than that of the specimens used in the tensile tests, a total of six samples from each group were tested. The flexural modulus (E_f), flexural strength (σ_f), and flexural strain (ε_f) were plotted and compared with

the FE results. The flexural modulus, flexural strength, and flexural strain of CFRP laminate were determined using Equations (5), (6), and (7) respectively.

$$E_f = \frac{L_s^3 F_{\max}}{4bh^3\left(\Delta\delta_{\max}\right)} \quad (5)$$

$$\sigma_f = \frac{3F_{\max}L_s}{2bd^2} \quad (6)$$

$$\varepsilon_f = \frac{6\left(\Delta\delta_{\max}\right)d}{L_s^2} \quad (7)$$

Here, F_{max}, $\Delta\delta_{max}$, b, h, and d represent the maximum force [N], maximum deflection [mm], width [mm], height [mm], and thickness [mm] of the CFRP beam, respectively.

V. COST ANALYSIS

The cost analysis was performed to identify that the commercial toaster oven used in VBO process is economical option to cure CFRP laminate compared with industrial-grade composite curing oven via the similar process and autoclave. The specification of the ovens and the cost data including the oven price and the electric consumption generated during each curing process were listed in Table 3. Due to the different size of three curing oven, we developed the definition of maximum production capacity of each oven to compare the production capacity in the similar scale. The maximum production capacity of each oven was defined as the ratio of the maximum size of CFRP laminate per one batch of production by the oven to the maximum achievable size of CFRP laminates produced by commercial toaster oven.

The electric consumption of the oven per one time of production, E_{oven} (kW·h), can be determined as follows:

$$E_{oven} = P_{oven} \times t_{curing} \quad (8)$$

where, P_{oven} and t_{curing} are electric power of the oven [kW] and total curing time of CFRP laminate [h], respectively.

Table 3: Specification and cost data of the ovens

	Autoclave oven*	Thermal convection ovens for VBO process	
		Industrial grade**	Toaster Oven
Internal dimensions [mm]	500x1,000	1,070×430 ×500	300×300 ×250
Weight [kg]	1,760	85	8
Total curing time/parts [min]	600	480	100
Power supply [V]	220	230	220
P_{OVEN} [kW]	25	2.2	1.5
Laminates size [mm]	760×420	740×370	240×120
Production capacity / batch [piece]	11	9	1
E_{OVEN} [kW·h]	250	17.6	2.5
C_E [$]	28.72	1.56	0.22
C_{OVEN} [$]	17,500	2,713.32	114.28

**Model NO. SN-CGF0510, Changzhou Sinomac Machinery Technology Co., Ltd., China*

***Model NO. OV301, Easy Composites Ltd., United Kingdom*

The electricity cost generated from the curing process, C_E [$], can be determined by multiplying the electric consumption of the oven per one time of production and the energy charge rate per one unit of electricity appliance, C_{unit} [$/kW·h]. Thus, it can be written as follows:

$$C_E = E_{oven} \times C_{unit} \quad (9)$$

According to the electricity tariffs in Thailand [31], for small business service, the rate of charge of the electric appliances are lower than 22 kV for first using of 0–150 kW·h and the next step of using of 151–400 kW·h is 0.08 $/kW·h and 0.11 $/kW·h, respectively. The businesses consuming the electricity more than 400 kW·h is charged with the fix rate of 0.12 $/kW·h.

The breakeven analysis was conducted to investigate the economical option between industrial curing and commercial toaster ovens. The oven cost was set as a

fixed cost and the electricity cost per one time of production was considered as variable cost. Thus, the total cost of the oven, $C_{T,\,oven}$, can be written as follows:

$$C_{T,oven} = C_{oven} + C_E x \begin{cases} Toaster\ oven: x = 1,2,3,...,n \\ Industrial\ oven: x = \left\lceil \frac{n}{9} \right\rceil \end{cases} \quad (10)$$

where, C_{oven} [$] and C_E [$] represent the oven cost and the electricity cost generated from the curing process by the ovens, respectively. x is the number of CFRP laminate produced by the ovens. For the commercial toaster oven, x is integer, which can be counted from 1, 2, 3, ..., to n pieces of laminate. For the industrial-grade composite curing oven, the electricity cost per one time of production remained constant regardless of the size and the number of CFRP laminate, therefore, x is limited by the maximum production, which was nine times larger than commercial toaster oven. Hence, to compare both ovens in the same scale of production, x was set as the round up of the ratio of the n pieces of laminate per one time of running the oven to the maximum production capacity of industrial-grade composite curing oven.

VI. RESULTS AND DISCUSSION

A. Surface Appearance and Through-thickness Voids of CFRP Laminates

The surface appearance of representative locations on the CFRP laminates was captured using a digital microscope as shown in Figures. 5a and 5b for the non-vacuum and vacuum specimens, respectively.

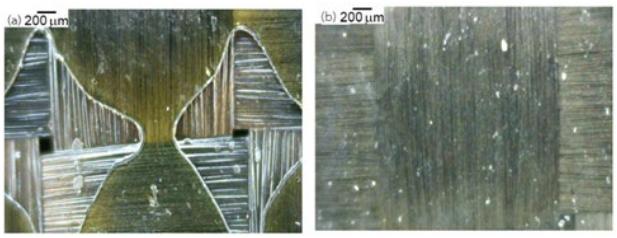

Figure 5: The surface appearance on the (a) non-vacuum and (b) vacuum CFRP specimens.

As expected, the sample cured under non-vacuum conditions exhibited a significant number of voids produced by air bubbles due to gas expansion as the oven was heated. Accordingly, the surface porosities of the non-vacuum specimen were observably higher than that of the vacuum specimen. In addition, uncured resin was observed at the cross-joint of the woven fiber in the non-vacuum specimen; this was not observed in the vacuum specimen. This suggests that a vacuum pressure of -1 bar allows the resin to fill the gaps between the fiber tow in the cross-joint network of the woven fiber prepreg even when utilizing a single cure cycle at 120°C with a dwell time of 50 minutes. Additional surface porosity generated by the presence of uncured resin at the cross-joints of the plain weave fiber is consistent with a previous study conducted by Hyun *et al.* [32]. The differences in surface porosities may influence the mechanical properties of the CFRP specimens; however, these porosities can be easily reduced or eliminated by grinding the sample using sandpaper [33]. Consequently, the increased surface porosities are typically treated as a minor problem when it comes to quality control. In contrast, the through-thickness voids in CFRP cannot be easily eliminated and are much harder to detect compared to surface porosity. Consequently, these voids are a major cause of failure in CFRP materials.

The distribution of the through-thickness voids as observed in the X-ray micro-CT 3D images extracted using ImageJ in both the non-vacuum and vacuum specimens are presented in Figures. 6a and 6b, respectively. The error (e) of the deviation of the void content in the small samples compared to the large samples was 0.53% at a scanning resolution of 12.0 µm. as calculated according to Equation (1). This indicates that the distribution of voids inside the sub-representative samples is uniform and sufficient to explain the distribution of void of the entire laminates The void

content in the non-vacuum and vacuum specimens was found to be 10.78 ± 0.001% and 0.297 ± 0.007%, respectively. The void content of the vacuum specimen was 96.95% less than that of the non-vacuum specimen, indicating that curing the specimens on the vacuum greatly reduced an amount of through-thickness voids in the samples. Furthermore, according to the Purslow's chart [34], the void content of the vacuum specimen would classify it under Grade B (very good quality), while the void content of the non-vacuum specimen would cause it to be classified as Grade F (very poor quality). These results show that high-quality CFRP specimens can be fabricated using a single cure cycle in a commercial toaster oven. The formation of through-thickness voids in the VBO process is generally due to one of two processes: 1) the insufficient impregnation of fibers before gelation, known as "flow-induced voids"; and 2) the presence of entrapped air, moisture, or resin volatiles, known as "gas-induced voids" [26].

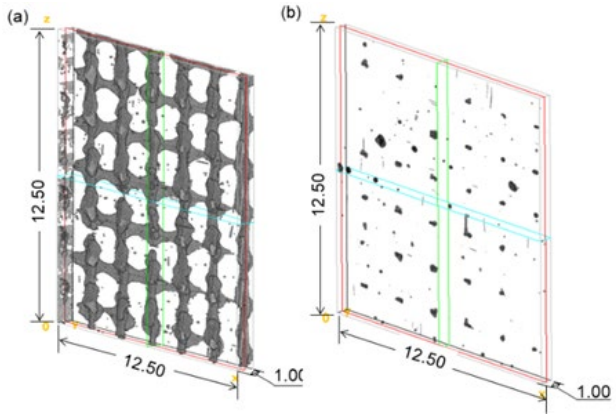

Figure 6: The distribution of through-thickness voids in a 3d view extracted from the X-ray micro-CT images using ImageJ: (a) non-vacuum specimens and (b) vacuum specimens.

Centea and Hubert reported that the vacuum pressures assisted with the evacuation of air, resulting in the reduction of gas-induced voids when subjected vacuum conditions at ambient temperatures [35]. As the temperature increases, the resin begins to flow, filling in the dry regions of the fiber tows, leading to a decrease in the number of flow-induced voids. Therefore, the surface appearance of CFRP in Figure 5 suggests that the VBO process conducted under vacuum conditions (-1 bar) was sufficient to suppress the formation of flow-induced voids but not gas-induced voids. This can be clearly seen by the absence of uncured resin in the cross-joints of the fiber as well as the lower surface porosities observed in the vacuum specimens (Figure 5b). The single cure cycle, conducted by heating the oven from room temperature to 120ºC at a ramp rate of 2.5ºC/min followed by 50 minutes of isothermal holding, improved the flow of resin through the dry area of the fiber tow. Thus, CFRP laminates could be achieved in a commercial toaster oven using a single cure cycle within short duration.

B. Mechanical Properties of the CFRP Specimen

To quantitatively assess the mechanical performance of CFRP laminates cured using a single cure cycle in a commercial toaster oven, the upper bounds of the following mechanical properties were determined using the results of a finite element model in which the presence of voids in the CFRP laminate was neglected. The von Mises stress distribution of the CFRP specimens under tension and three-point bending load as obtained from the results of the finite element modeling are presented in Figures. 7a and 7b, respectively. These results were compared to the mechanical properties of the CFRP vacuum specimens as obtained from tensile and three-point bending tests (Figures. 7c and 7d, respectively).

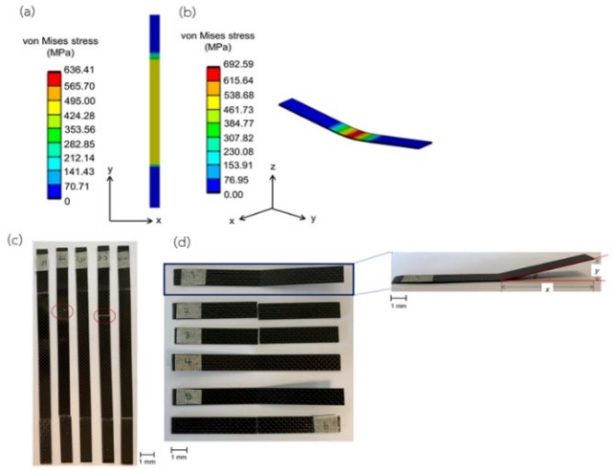

Figure 7: Stress distribution by FEA: (a) under tension; (b) under three-point bending. The fractured specimens obtained after (c) the tensile test and (d) the three-point bending test.

Figure 7a shows that the CFRP laminate was capable of withstanding a maximum stress of 424.28–495.00 MPa (yellow contour) at the gauge length before the specimen failed under the Tsai-Wu criteria. This suggests that, theoretically, fractures should occur around the gauge length. Experimentally, it was found that vacuum specimens #2 and #4 failed at the gauge length, consistent with the results of the simulation, while the other samples failed near the grips. Figure 7b shows that the middle of the CFRP beam (the location of the load) was subjected to a maximum stress ranging from 615.64–692.59 MPa (red contour) before it failed under Tsai-Wu criteria. In the three-point bending test, three vacuum specimens (specimens #2, #3 and #6) ruptured in the middle of the beam, while the other three specimens (specimens #1, #4 and #5) failed on the outer surface of the middle of the beam without breaking into two parts (Figure 7d). All six vacuum specimens subjected to the three-point bending test failed at the point of loading (mid-span), consistent with the location of the greatest accumulated stress (red contour) as predicted by the finite element model (Figure 7b). The average value of the bending angle (°) at failure, which calculated from specimens which failed on the outer surface as shown in Figure 7d was found to be 10.56°.

Table 4 summarizes the mechanical properties, void content and part quality based on Purslow's chart of CFRP laminates under tension and flexural loading in three cases: Vacuum, non-vacuum and FE analysis. Full detial of stress-strain curves CFRP under tensile and three-point bending tests are depicted in Figures. 8a and 8b, respectively. Values are plotted in mean ± SD, calculated from six replications.

Table 4: Mechanical properties, void content and part quality of CFRP laminates: Vacuum, non-vacuum and FE analysis

Properties	Vacuum	Non-vacuum	FE model
Through-thickness void [%]	0.297 ± 0.007	10.78 ± 0.001	N/A
Tensile modulus [GPa]	41.91 ± 0.19	35.98 ± 1.65	42.13
Tensile strength [MPa]	451.02 ± 11.78	344.04 ± 37.00	473.49
Elongation [%]	1.10 ± 0.03	0.90 ± 0.10	1.12
Flexural modulus [GPa]	42.26 ± 1.46	31.10 ± 2.13	35.82
Flexural strength [MPa]	767.61 ± 19.43	363.89 ± 26.18	734.16
Deformation [%]	1.8 ± 1.94	0.95 ± 0.14	2.05
Achievable thickness [mm]	0.97 ± 0.01	1.15 ± 0.01	1
Part quality based on Purslow's chart	B (very good quality)	F (very poor quality)	Ideal case

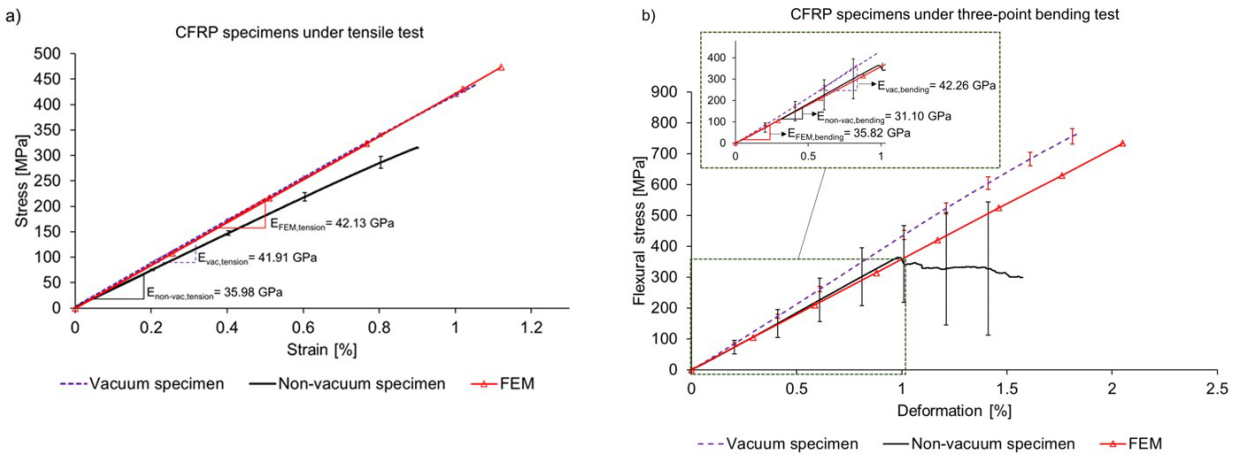

Figure 8: Stress-strain curves of CFRP laminates under (a) tensile and (b) three-point bending tests.
Values presented are the average along with error bars determined from the standard deviation (SD) of six replications.

Figure 8a shows the good agreement, 4.8% difference, between stress-strain curves of vacuum specimen (dashed purple line), and FE simulation result (red line with triangle). It is obvious that the stress-strain curve of vacuum CFRP is in good agreement with FE results, indicating that proposed single curing cycle in commercial toaster oven can achieve the maximum performance under tension.

On the other hand, non-vacuum CFRP specimen (black line) exhibited the lowest Young's modulus, 35.98 GPa, and tensile strength, 344.04 MPa. The non-vacuum CFRP samples—which had the highest void contents—exhibited a 27.38% and 14.90% decrease in ultimate tensile strength and tensile modulus compared to the FEM results, respectively. These results suggest that, in the context of tensional loading, CFRP specimens prepared under vacuum and cured using a single cure cycle in a commercial toaster oven can achieve mechanical properties that are close to the maximum theoretical mechanical performance.

Figure 8b shows the stress-strain curve of vacuum (dashed purple line), non-vacuum (black line), and FE results (red line with a triangle) of CFRP laminates under a three-point bending test. Despite the close value of flexural modulus of the non-vacuum specimen and simulation result, the non-vacuum specimen broke at 0.95% flexural strain and achieved 363.89 MPa of flexural strength. The flexural strength and percentage of deformation of CFRP under three-point bending obtained from FE results was higher than in non-vacuum specimenss. Regarding Table 4, flexural strength and deformation of simulation result were less than 12.12% difference compared to the vacuum specimen. When the specimens were under flexural test, both compression and tension load occurred, and most of them fractured at the tension load side. Figure 7d showed the fracture pattern of CFRP laminate under flexural loading, indicating the fracture along the tension side. Thus, it can be implied that non-vacuum CFRP specimens failed at the tension side, resulting in the lowest flexural strength and strain. One of the major factors influencing the flexural strength and modulus is the presence of voids. The rapid decrease in flexural strength of unidirectional CFRP laminates as the void content of the material increased was previously reported by Liu *et al.* [13]. It is thus important to note the flexural strength of the CFRP laminates was considered more sensitive to the presence of voids than other similar mechanical properties.

C. Cost Estimation and Breakeven Analysis for Manufacturing CFRP Using Commercial Toaster Oven

In the case of fabrication of CFRP laminate with similar size, the electricity cost per piece of CFRP laminate generated by autoclave was the highest, 2.61$/piece, whereas, the commercial toaster and industrial-grade composite curing ovens exhibited 0.22$/piece and 0.17$/piece, respectively. The cost per piece of CFRP was the highest in autoclave process; however, the electricity cost per piece of CFRP laminate produced by commercial toaster oven in one time of operation was higher than that industrial-grade of composite curing ovens. To strategically compare type of oven, a break-even analysis is conducted. Here, a common variable for the analysis is the number of production quantities, and the dependent variable is the total cost of each alternative. The result of the break-even analysis is illustrated in Figure 9. The total cost of commercial toaster oven and industrial-grade composite curing oven are represented by the green line and the purple line, respectively. The break-even point occurs at a production quantity of 54,035 pieces. Consequently, if the demand for the CFRP laminate is greater than 54,035 pieces, the industrial-grade composite curing oven should be selected for VBO process since the total cost is lower.

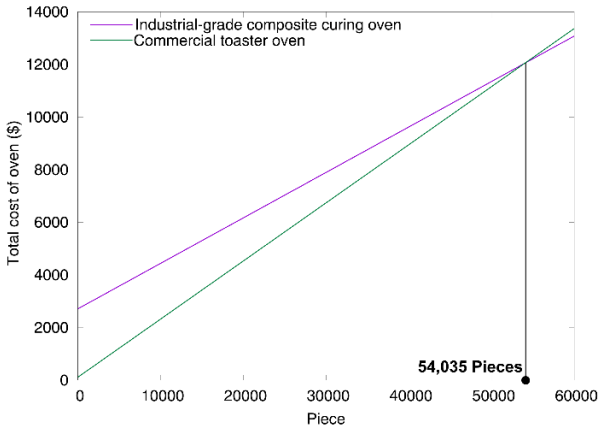

Figure 9: The total cost of the commercial toaster oven and industrial-grade composite curing oven.

In case industrial-grade composite curing and commercial toaster ovens are supposed to be used to fabricate similar sizes of CFRP parts using VBO process, the commercial toaster oven is more economical than the industrial-grade composite curing oven when a moderate production capacity is required. Furthermore, the required space for the installation of a commercial toaster oven is small as its size is compact. Hence, the commercial toaster oven used to cure CFRP laminate via VBO process is adequate in terms of high-quality CFRP laminate production and cost-effective solution for the small-scale companies, which have moderate production capacity and space for an installation is limited.

VII. LIMITATION OF THE STUDY

The results in this study are discussed based on the 23-litre size of commercial toaster ovens or smaller in which their functions are simple to operate and they can be easily found at department stores at affordable prices. However, various classifications of commercial toaster ovens that have more functions with larger sizes than the one used in this study. Therefore, the mechanical properties of CFRP and cost analysis in this study may not apply to the large-scale CFRP laminate and production capacity. Besides, the single-step curing proposed in this study can be applied up to four to eight plie, 2–3 mm CFRP thickness. The curing conditions of single-step curing should be further investigated for the greater CFRP thickness.

VIII. CONCLUSION

This study has successfully demonstrated that CFRP laminates with good mechanical properties and low void contents can be fabricated using a VBO process with a single cure cycle in a commercial toaster oven, providing an alternative, cost-effective manufacturing CFRP laminates for small entrepreneurs. The cost analysis

is carried out to investigate the cost-effective point of using a commercial toaster oven compared with using an industrial-grade composite curing oven in VBO and autoclave processes. A FE model, which neglected the presence of voids, was used to estimate the maximum theoretical mechanical performance of the CFRP laminates. The results of this study can be summarized as follows:

(i) X-ray micro-CT 3D images revealed that the through-thickness void contents of the vacuum and non-vacuum specimens were 0.28% and 10.78%, respectively. Thus, according to Purslow's chart, the specimen prepared under vacuum conditions could be classified as Grade B (very good quality), while the non-vacuum specimen could only be classified as Grade F (very poor quality).

(ii) The average tensile strength, modulus and percent elongation at break of CFRP specimens prepared under vacuum were 451.02 MPa, 41.90 GPa, and 1.10%, respectively; these values were approximately 4.8% less than the FE simulation results. In contrast, the non-vacuum specimen exhibited an average tensile strength, tensile modulus, and percent elongation at break of 344 MPa, 35.98 GPa, and 0.99%. This suggests that the presence of voids in CFRP laminates can reduce tensile strength and modulus by 27.38% and 14.90%, respectively. Thus, in the context of tensional loading, specimens prepared under vacuum using a VBO process with a single cure cycle in a commercial toaster oven can produce CFRP laminates with high mechanical performances. On the other hand, high void content presenced in non-vacuum specimen gradually deceased 52.59% of flexural strength compared to vacuum specimen and simulation results. Non-vaccum specimen fractured at 0.95% deflection whereas vacuum specimen and simulation results broke at 1.8% and 2.05%, respectively. This indicates that the flexural strength of the CFRP laminates was extremely sensitive to even small void contents, correspoinding to published work [13].

(iii) The single-step cure cycle in commercial toaster oven allows for curing time of less than 100 minutes, which is almost 10 times less than the total curing time of multiple-step cure cycle operated by an autoclave and an industrial-grade composite curing oven in VBO process. Therefore, the energy consumption for total cure cycle using commercial toaster oven is the lowest, 2.5 kW·h. The break-even analysis disclosed that the commercial toaster oven would be economical option for a moderate capacity of production, 54,000 pieces, when the similar size of samples was considered. Consequently, the commercial toaster oven is recommended for implementation in VBO process for a small business that demands moderate production capacity and high-quality CFRP laminates. Additionally, the commercial toaster oven is installed easily in a limited space due to compact size, making it logistically convenient for many users

ACKNOWLEDGEMENT

This work was supported by Thai-Nichi Institute of Technology, grant numbers 2102/A004 and 2306/A001. The authors would like to acknowledge the financial support of the Department of Research and Innovation, Thai-Nichi Institute of Technology. We are also thankful to Mr. P. Prommachat for the fabrication of the CFRP laminate.

REFERENCES

[1] J. T. J. Burd, E. A. Moore, H. Ezzat, R. Kirchain, and R. Roth, "Improvements in electric vehicle battery technology influence vehicle lightweighting and material substitution decisions," *Appl. Energy,* vol. 283, Feb. 2021, Art. no. 116269, doi: 10.1016/j.apenergy.2020.116269.

[2] B. Shaffer, M. Auffhammer, and C. Samaras, "Make electric vehicles lighter to maximize climate and safety benefits," *Nature,* vol. 598, pp. 254–256, Oct. 2021, doi: 10.1038/d41586-021-02760-8.

[3] T. Ishikawa *et al.*, "Overview of automotive structural composites technology developments in Japan," *Compos. Sci. Technol.,* vol. 155, pp. 221–246, Feb. 2018, doi: 10.1016/j.compscitech.2017.09.015.

[4] M. R. Bambach, M. Elchalakani, and X. L. Zhao, "Composite steel-CFRP SHS tubes under axial impact," *Compos. Struct.,* vol. 87, no. 3, pp. 282–292, Feb. 2009, doi: 10.1016/j.compstruct.2008.02.008.

[5] Q. Liu, Y. Lin, Z. Zong, G. Sun, and Q. Li, "Lightweight design of carbon twill weave fabric composite body structure for electric vehicle," *Compos. Struct.,* vol. 97, pp. 231–238, Mar. 2013, doi: 10.1016/j.compstruct.2012.09.052.

[6] J.-M. Lee, B.-J. Min, J.-H. Park, D.-H. Kim, B.-M. Kim, and D.-C. Ko, "Design of lightweight CFRP automotive part as an alternative for steel part by thickness and lay-up optimization," *Materials,* vol. 12, no. 14, Jul. 2019, Art. no. 2309, doi: 10.3390/ma12142309.

[7] J. Hu, X. Deng, X. Zhang, W. X. Wang, and T. Matsubara, "Effect of off-axis ply on tensile properties of $[0/\theta]_{ns}$ thin ply laminates by experiments and numerical method," *Polymers,* vol. 13, no. 11, May 2021, Art. no. 1809, doi: 10.3390/polym13111809.

[8] M. Kawai and T. Taniguchi, "Off-axis fatigue behavior of plain weave carbon/epoxy fabric laminates at room and high temperatures and its mechanical modeling," *Compos. Part A: Appl. Sci. Manuf.,* vol. 37, no. 2, pp. 243–256, Feb. 2006, doi: 10.1016/j.compositesa.2005.07.003.

[9] S. Y. Park, C. H. Choi, W. J. Choi, and S. S. Hwang, "A comparison of the properties of carbon fiber epoxy composites produced by non-autoclave with vacuum bag only prepreg and autoclave process," *Appl. Compos. Mater.,* vol. 26, pp. 187–204, Feb. 2019, doi: 10.1007/s10443-018-9688-y.

[10] D. Saenz-Castillo, M. I. Martín, S. Calvo, F. Rodriguez-Lence, and A. Güemes, "Effect of processing parameters and void content on mechanical properties and NDI of thermoplastic composites," *Compos. Part A: Appl. Sci. Manuf.,* vol. 121, pp. 308–320, Jun. 2019, doi: 10.1016/j.compositesa.2019.03.035.

[11] P. Olivier, J. P. Cottu, and B. Ferret, "Effects of cure cycle pressure and voids on some mechanical properties of carbon/epoxy laminates," *Composites,* vol. 26, no. 7, pp. 509–515, Jul. 1995, doi: 10.1016/0010-4361(95)96808-J.

[12] M. Bodaghi, C. Cristóvão, R. Gomes, and N. C. Correia, "Experimental characterization of voids in high fibre volume fraction composites processed by high injection pressure RTM," *Compos. Part A: Appl. Sci. Manuf.,* vol. 82, pp. 88–99, Mar. 2016, doi: 10.1016/j.compositesa.2015.11.042.

[13] L. Liu, B. M. Zhang, D. F. Wang, and Z. J. Wu, "Effects of cure cycles on void content and mechanical properties of composite laminates," *Compos. Struct.,* vol. 73, no. 3, pp. 303–309, Jun. 2006, doi: 10.1016/j.compstruct.2005.02.001.

[14] K. S. Madhok, "Comparative characterization of out-of-autoclave materials made by automated fiber placement and hand-lay-up processes," M.S. thesis, Dept. Mech. Ind. Eng., Concordia Univ., Montreal, Cananda, 2013. [Online]. Available: http://spectrum.library.concordia.ca/978552/1/Madhok_MASc_S2014.pdf

[15] T. Centea and S. R. Nutt, "Manufacturing cost relationships for vacuum bag-only prepreg processing," *J. Compos. Mater.,* vol. 50, no. 17, pp. 2305–2321, 2015, doi: 10.1177/0021998315602949.

[16] R. A. Witik, F. Gaille, R. Teuscher, H. Ringwald, V. Michaud, and J.-A. E. Månson, "Economic and environmental assessment of alternative production methods for composite aircraft components," *J. Cleaner Prod.*, vol. 29–30, pp. 91–102, Jul. 2012, doi: 10.1016/j.jclepro.2012.02.028.

[17] *Matrix TDS–Technical Data Sheet DT806 Resins*, Delta-Tech., Lucca, Italy, 2014.

[18] J. Galos, "Microwave processing of carbon fibre polymer composites: a review," *Polym. Polym. Compos.*, vol. 29, no. 3, pp. 151–162, 2021, doi: 10.1177/0967391120903894.

[19] H. Koushyar, S. Alavi-Soltani, B. Minaie, and M. Violette, "Effects of variation in autoclave pressure, temperature, and vacuum-application time on porosity and mechanical properties of a carbon fiber/epoxy composite," *J. Compos. Mater.*, vol. 46, no. 16, pp. 1985–2004, 2011, doi: 10.1177/0021998311429618.

[20] Y. Alekajbaf, S. Murali, and D. Dancila, "Energy efficient microwave curing of carbon fiber reinforced polymer via metamaterial matching and advanced electromagnetic exposure control," *Int. J. Microw. Wireless Technol.*, pp.1–7, 2024, doi: 10.1017/S1759078724000072.

[21] M. Kwak, P. Robinson, A. Bismarck, and R. Wise, "Microwave curing of carbon–epoxy composites: Penetration depth and material characterisation," *Compos. Part A: Appl. Sci. Manuf.*, vol. 75, pp. 18–27, Aug. 2015, doi: 10.1016/j.compositesa.2015.04.007.

[22] K. B. Katnam, A. J. Comer, D. Roy, L. F. M. da Silva, and T. M. Young, "Composite repair in wind turbine blades: An overview," *J. Adhes.*, vol. 91, no. 1–2, pp. 113–139, 2015, doi: 10.1080/00218464.2014.900449.

[23] D. B. Bender, T. Centea, and S. Nutt, "Fast cure of stable semi-pregs via VBO cure," *Adv. Manuf. Polym. Compos. Sci.*, vol. 6, no. 4, pp. 245–255, 2020, doi: 10.1080/20550340.2020.1869891.

[24] Y. Li, N. Li, J. Zhou, and Q. Cheng, "Microwave curing of multidirectional carbon fiber reinforced polymer composites," *Compos. Struct.*, vol. 212, pp. 83–93, Mar. 2019, doi: 10.1016/j.compstruct.2019.01.027.

[25] T.-H. Hou. *Cure cycle design methodology for fabricating reactive resin matrix fiber reinforced composites: - A protocol for producing void-free quality laminates*. (2014). [Online]. Available: https://ntrs.nasa.gov/api/citations/20140012782/downloads/20140012782.pdf

[26] M. Mehdikhani, L. Gorbatikh, I. Verpoest, and S. V. Lomov, "Voids in fiber-reinforced polymer composites: A review on their formation, characteristics, and effects on mechanical performance," *J. Compos. Mater.,* vol. 53, no. 12, pp. 1579–1669, 2018, doi: 10.1177/0021998318772152.

[27] A. R. Chambers, J. S. Earl, C. A. Squires, and M. A. Suhot, "The effect of voids on the flexural fatigue performance of unidirectional carbon fibre composites developed for wind turbine applications," *Int. J. Fatigue,* vol. 28, no. 10, pp. 1389–1398, Oct. 2006, doi: 10.1016/j.ijfatigue.2006.02.033.

[28] D. Zhang, D. Heider, and J. W. Gillespie, "Determination of void statistics and statistical representative volume elements in carbon fiber-reinforced thermoplastic prepregs," *J. Thermoplast. Compos. Mater.,* vol. 30, no. 8, pp. 1103–1119, 2015, doi: 10.1177/0892705715618002.

[29] *Standard Test Method for Tensile Properties of Polymer Matrix Composite Materials*, ASTM Standard D3039/D3039M-00, 2002.

[30] *Standard Test Methods for Flexural Properties of Unreinforced and Reinforced Plastics and Electrical Insulating Materials,* ASTM Standard D790-03, 2002.

[31] "Electricity tariffs (January 2023)," Provincial Electricity Authority (PEA), Bangkok, Thailand, 2023. [Online]. Available: https://www.pea.co.th/en/electricity-tariffs

[32] D.-K. Hyun, D. Kim, J. H. Shin, B.-E. Lee, D.-H. Shin, and J. H. Kim, "Cure cycle modification for efficient vacuum bag only prepreg process," *J. Compos. Mater.,* vol. 55, no. 8, pp. 1039–1051, 2021, doi: 10.1177/0021998320963541.

[33] H. Sasahara, T. Kikuma, R. Koyasu, and Y. Yao, "Surface grinding of carbon fiber reinforced plastic (CFRP) with an internal coolant supplied through grinding wheel," *Precis. Eng.,* vol. 38, no. 4, pp. 775–782, Oct. 2014, doi: 10.1016/j.precisioneng.2014.04.005.

[34] D. Purslow, "On the optical assessment of the void content in composite materials," *Composites,* vol. 15, no. 3, pp. 207–210, Jul. 1984, doi: 10.1016/0010-4361(84)90276-3.

[35] T. Centea and P. Hubert, "Measuring the impregnation of an out-of-autoclave prepreg by micro-CT," *Compos. Sci. Technol.,* vol. 71, no. 5, pp. 593–599, Mar. 2011, doi: 10.1016/j.compscitech.2010.12.009.